Electronic Supplementary Material (ESI) for Journal of Materials Chemistry A.

Electronic Supplementary Information

Highly efficient artificial light-harvesting system with two-step sequential energy transfer based on supramolecular self-assembly

Guangping Sun,[a] Weirui Qian,[a] Jianmin Jiao,[a] Tingting Han,[c] Yukun Shi,[a] Xiao-Yu Hu*[b] and Leyong Wang*[a,d]

[a] *Key Laboratory of Mesoscopic Chemistry of MOE, Jiangsu Key Laboratory of Advanced Organic Materials, School of Chemistry and Chemical Engineering, Nanjing University, Nanjing, 210023, China.*

[b] *College of Material Science and Technology, Applied Chemistry Department, Nanjing University of Aeronautics and Astronautics, Nanjing, 211100, China.*

[c] *State Key Laboratory of Analytical Chemistry for Life Science, School of Chemistry and Chemical Engineering, Nanjing University, Nanjing 210023, China.*

[d] *School of Petrochemical Engineering, Changzhou University, Changzhou, 213164, China.*

* *Corresponding author: huxy@nuaa.edu.com (X.-Y. Hu); lywang@nju.edu.com (L. Wang).*

Table of Contents

1. General information and experimental procedure

1) General information:

All reactions were performed in air atmosphere unless otherwise stated. The commercially available reagents and solvents were either employed as purchased or dried according to procedures described in the literatures. Column chromatography was performed with silica gel (200 – 300 and 300 – 400 mesh) produced by Qingdao Marine Chemical Factory, Qingdao (China). All yields were given as isolated yields. NMR spectra were recorded on a Bruker DPX 400 MHz spectrometer with internal standard tetramethylsilane (TMS) and solvent signals as internal references at room temperature, and the chemical shifts (δ) were expressed in ppm and *J* values were given in Hz. High-resolution electrospray ionization mass spectra (HR-ESI-MS) were recorded on an Agilent 6540Q-TOF LCMS equipped with an electrospray ionization (ESI) probe operating in the positive-ion mode with direct infusion. Transmission electron microscope (TEM) investigations were carried out on a JEM-2100 instrument. Dynamic light scattering (DLS) measurements were carried out on a Brookhaven BI-9000AT system (Brookhaven Instruments Corporation, USA), using a 200-mW polarized laser source (λ = 514 nm). Zeta-potential measurements were performed at 25 °C on a Zetasizer Nano Z apparatus (Malvern Instruments Ltd., UK) using the Smoluchowski model for the calculation of the Zeta-potential from the measured electrophoretic mobility. The UV-Vis absorption spectra were measured on a Perkin Elmer Lambda 35 UV-Vis Spectrometer. The ITC experiment was performed on an ITC 200 micro-calorimeter (GE Company, USA). The excitation and emission spectra were recorded on a Hitachi F-7000 Fluorescence Spectrometer. The fluorescence lifetimes were measured employing time correlated single photon counting on a FLS980 instrument (Edinburg Instruments Ltd., Livingstone, UK) with a pulsed xenon lamp. The quantum yields were carried out on a FLS980 instrument with the integrating sphere.

2) Experimental procedure:

Fabrication of supramolecular nanoparticle solution. Initially, the stock solution of **BPT** (0.02 M, dissolved in DMSO), **WP5** (4.2×10^{-4} M, dissolved in water), **DBT** (2×10^{-4} M, dissolved in DMSO), and **NiR** (2×10^{-4} M, dissolved in DMSO) were prepared, respectively. **WP5⊃BPT** nanoparticles were prepared as follows: 25 μL of **BPT** solution and 240 μL of **WP5** solution were added into 4.76 mL of water. **WP5⊃BPT-DBT** nanoparticles were prepared as follows: 25 μL of **BPT** solution, 7 μL of **DBT** solution, and 240 μL of **WP5** solution were added into 4.76 mL of water. **WP5⊃BPT-DBT-NiR** nanoparticles were prepared as follows: 25 μL of **BPT** solution, 7 μL of **DBT** solution, 5.3 μL of **NiR** solution, and 240 μL of **WP5** solution were added into 4.76 mL of water.

2. Synthesis of host molecule WP5 and guest molecule BPT

1) Synthesis of host molecule WP5

WP5 was synthesized and purified according to previously reported procedures (**Fig. S1**).[S1–S6]

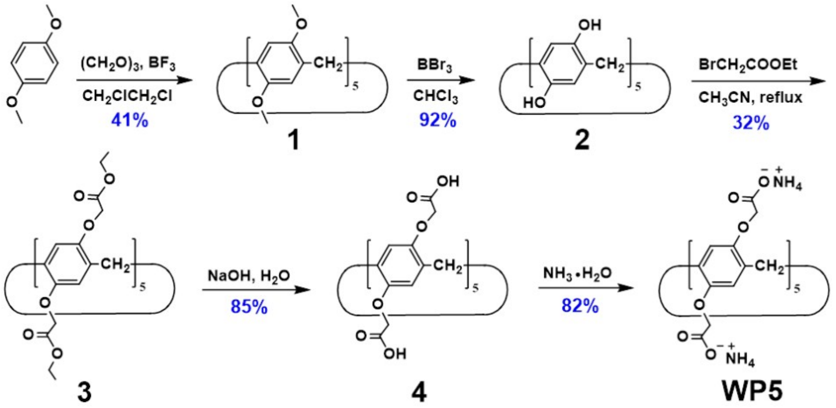

Fig. S1 Synthesis route of host molecule **WP5.**

2) Synthesis of guest molecule BPT

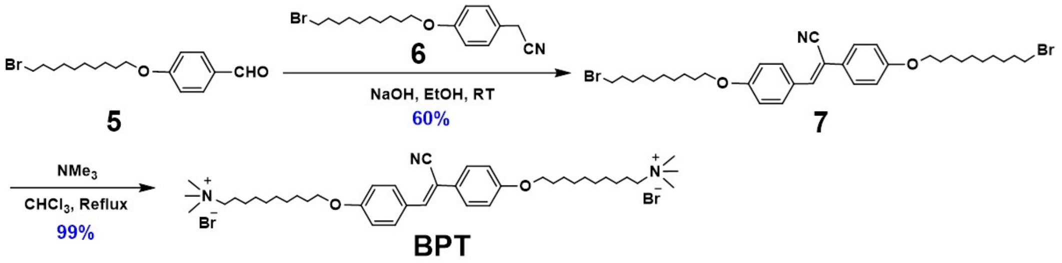

Fig. S2 Synthesis route of guest molecule **BPT.**

Synthesis of compound 5[S7]

4-Hydroxybenzaldehyde (0.74 g, 6.0 mmol) and 1,10-dibromodecane (3.56 g, 12 mmol) was refluxed in the presence of K_2CO_3 (1.44 g, 10.4 mmol) in dry acetonitrile (120 mL) for 24 h under argon. After the reaction mixture was cooled to room temperature, the solid was filtered and the filtrate was concentrated under vacuum. The obtained crude product was then purified by flash chromatography (petroleum ether : ethyl acetate = 10:1, *v/v*) to give compound **5** as a white crystalline solid (1.22 g, 3.6 mmol, 60%). ^{1}H NMR ($CDCl_3$, 400 MHz, 298 K) δ (ppm): 9.88 (s, 1H), 7.84 (d, J = 6.8 Hz, 2H), 7.00 (d, J = 7.2 Hz, 2H), 4.06 (t, J = 6.8 Hz, 2H), 3.43 (t, J = 7.2 Hz, 2H), 1.87 – 1.78 (m, 4H), 1.47 – 1.43 (m, 4H), 1.39 – 1.31 (m, 8H).

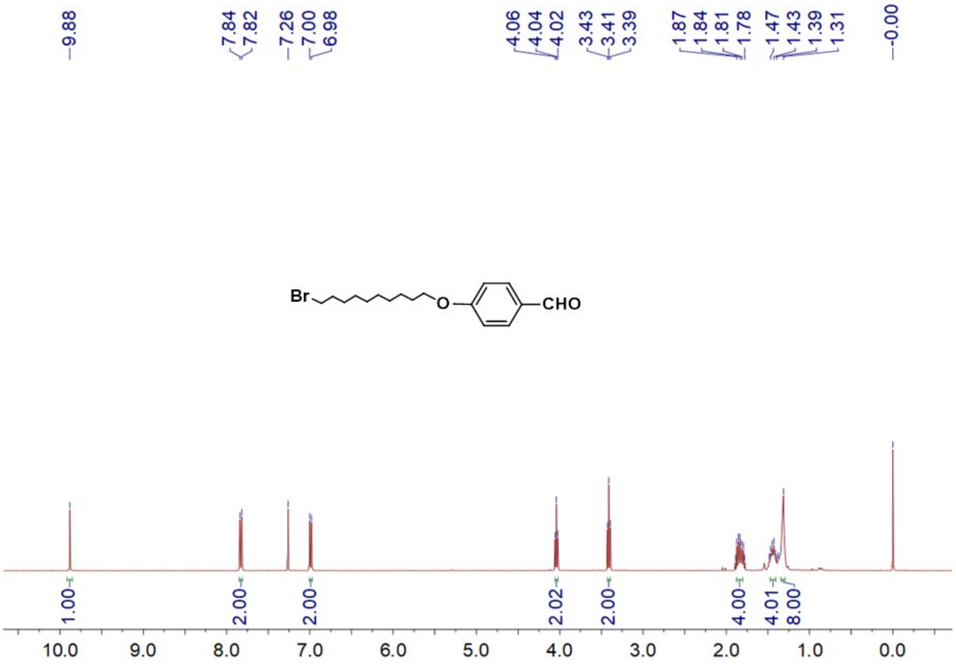

Fig. S3 ^{1}H NMR spectrum (400 MHz, CDCl$_3$, 298 K) of compound **5**.

Synthesis of compound 6[S8]

4-Hydroxybenzyl cyanide (0.8 g, 6.0 mmol) and 1,10-dibromodecane (3.56 g, 12 mmol) was refluxed in the presence of K_2CO_3 (1.44 g, 10.4 mmol) in dry acetonitrile (120 mL) for 24 h under argon. After the reaction mixture was cooled to room temperature, the solid was filtered and the filtrate was concentrated under vacuum. The obtained crude product was then purified by flash chromatography (petroleum ether : ethyl acetate = 10:1, *v/v*) to give compound **6** as a white crystalline solid (1.37 g, 3.9 mmol, 65%). ^{1}H NMR (CDCl$_3$, 400 MHz, 298 K) δ (ppm): 7.23 (d, *J* = 8.4 Hz, 2H), 6.90 (d, *J* = 8.8 Hz, 2H), 3.96 (t, *J* = 6.8 Hz, 2H), 3.60 (s, 2H), 3.43 (t, *J* = 6.8 Hz, 2H), 1.87 – 1.74 (m, 4H), 1.43 – 1.36 (m, 4H), 1.31 – 1.28 (m, 8H).

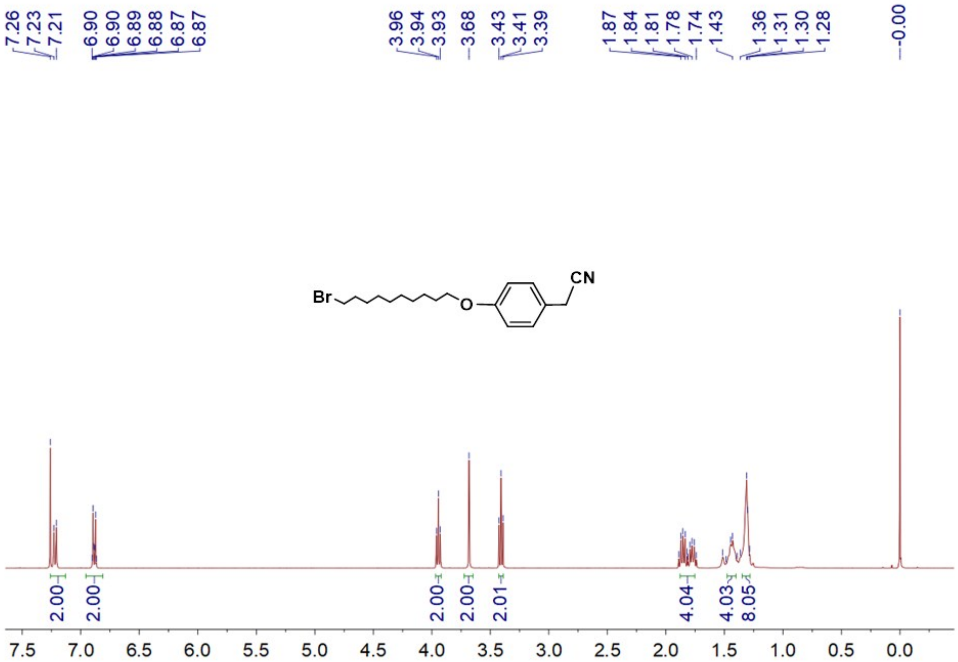

Fig. S4 ^{1}H NMR spectrum (400 MHz, CDCl$_3$, 298 K) of compound **6**.

Synthesis of compound 7

Compound **5** (0.1 g, 0.29 mmol) and compound **6** (0.1 g, 0.29 mmol) were added to a solution of tetrabutylammonium hydroxide (5 drop, 25%) in ethanol (20 mL), and then the mixture was refluxed for 12 h under argon. After cooling, the mixture was filtered and the solid was washed with ethanol to afford compound **7** as a white solid (0.11 g, 0.17 mmol, 60%). ^{1}H NMR (CDCl$_3$, 400 MHz, 298 K) δ (ppm): 7.84 (d, *J* = 8.8 Hz, 2H), 7.55 (d, *J* = 9.2 Hz, 2H), 7.34 (s, 1H), 6.96 – 6.92 (m, 4H), 4.03 – 3.97 (m, 4H), 3.43 (t, *J* = 6.8 Hz, 4H), 1.86 – 1.76 (m, 8H), 1.47 – 1.32 (m, 24H). ^{13}C NMR (100 MHz, CDCl$_3$, 298 K) δ (ppm): 160.7, 159.7, 139.9, 130.9, 127.0, 126.6, 118.8, 114.9, 114.8, 108.2, 68.2, 34.0, 32.8, 29.42, 29.35, 29.3, 29.2, 28.7, 28.2, 26.0. HR-ESI-MS: m/z [M + H]$^+$ calcd for [C$_{35}$H$_{50}$Br$_2$NO$_2$]$^+$ 678.2162, found 678.2141, m/z [M + Na]$^+$ calcd for [C$_{35}$H$_{49}$Br$_2$NNaO$_2$]$^+$ 700.1981, found 700.1985.

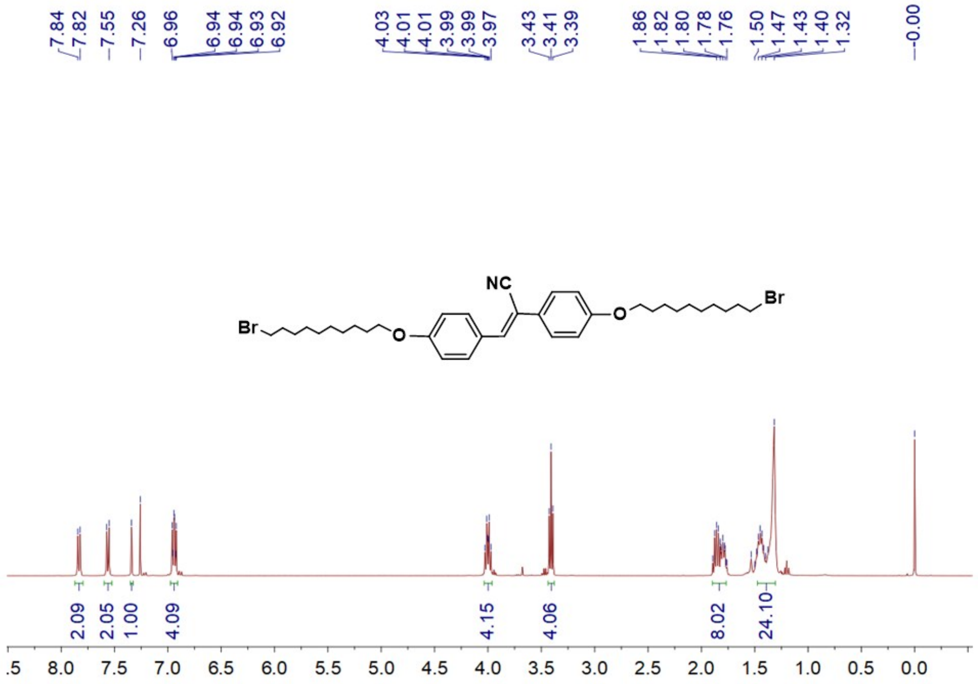

Fig. S5 ^{1}H NMR spectrum (400 MHz, CDCl$_3$, 298 K) of compound **7**.

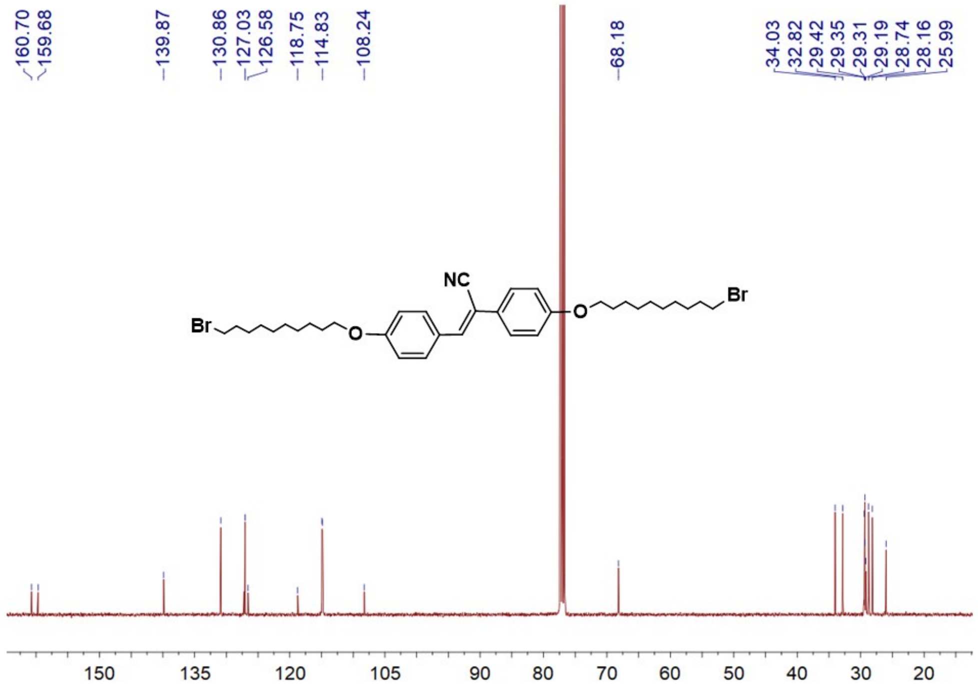

Fig. S6 ^{13}C NMR spectrum (400 MHz, CDCl$_3$, 298 K) of compound **7**.

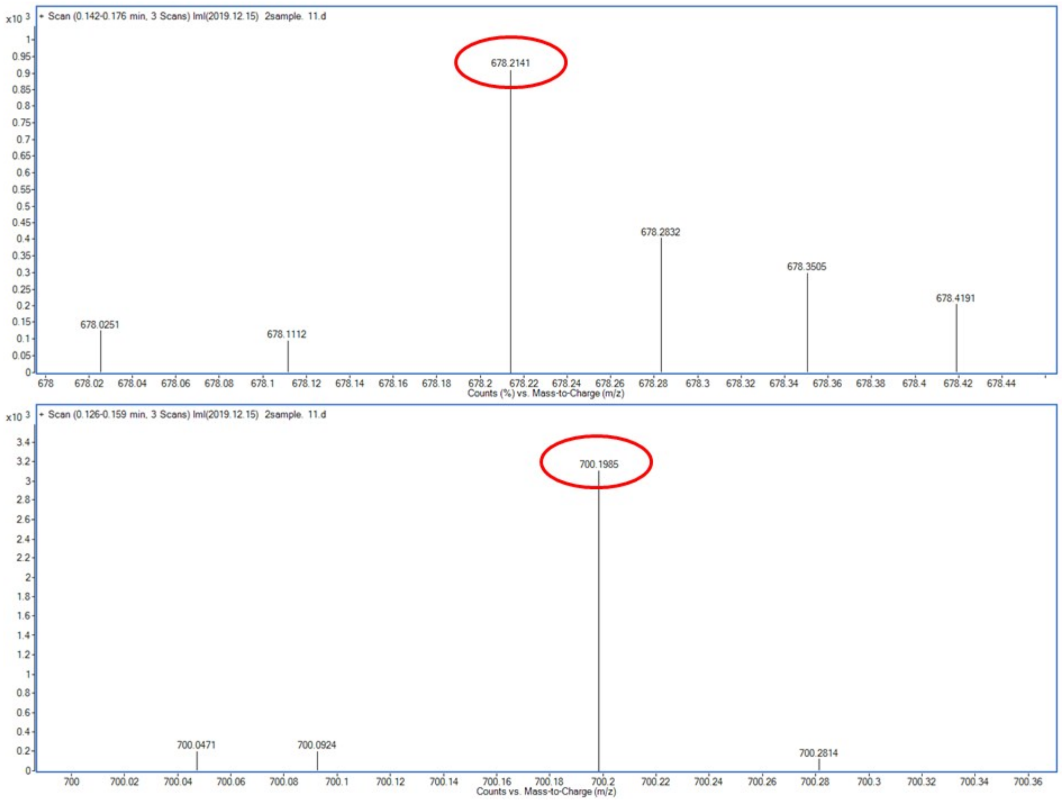

Fig. S7 HR-ESI-MS spectra of compound **7**.

Synthesis of compound BPT

Compound **7** (0.59 g, 0.88 mmol) was dissolved in chloroform (15 mL) and trimethylamine (0.74 g, 12.6 mmol) was added. The mixture was refluxed for 12 h. Then, the reaction mixture was concentrated under reduced pressure and diethyl ether (30 mL) was added. The precipitates was collected by filtration, washed by diethyl ether and dried in vacuum to afford compound **BPT** as a white solid (0.69 g, 0.87 mmol, 99%). ^{1}H NMR (400 MHz, DMSO-d_6, 298 K) δ (ppm): 7.89 (d, J = 8.8 Hz, 2H), 7.82 (s, 1H), 7.66 (d, J = 8.8 Hz, 2H), 7.08 (dd, J = 12.8, 8.8 Hz, 4H), 4.06 – 4.00 (m, 4H), 3.27 – 3.20 (m, 4H), 3.05 (s, 18H), 1.73 – 1.65 (m, 8H), 1.43 – 1.41 (m, 4H), 1.31 – 1.27 (m, 20H). ^{13}C NMR (100 MHz, DMSO-d_6, 298 K) δ (ppm): 160.7, 159.6, 140.7, 131.3, 127.3, 126.8, 119.0, 115.5, 115.3, 107.1, 68.2, 65.7, 52.5, 29.4, 29.2, 29.1, 29.03, 28.96, 26.2, 26.0, 22.5. HR-ESI-MS: m/z $[M - 2Br]^{2+}$ calcd for $[C_{41}H_{67}N_3O_2]^{2+}$ 316.7611, found 316.7614.

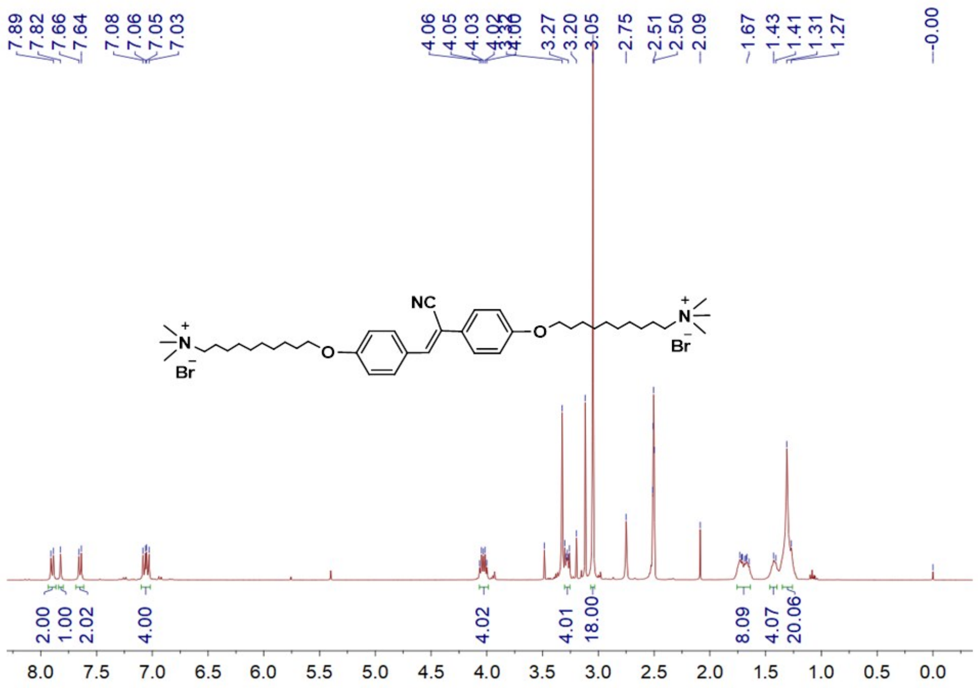

Fig. S8 ^{1}H NMR spectrum (400 MHz, DMSO-d_6, 298 K) of compound **BPT**.

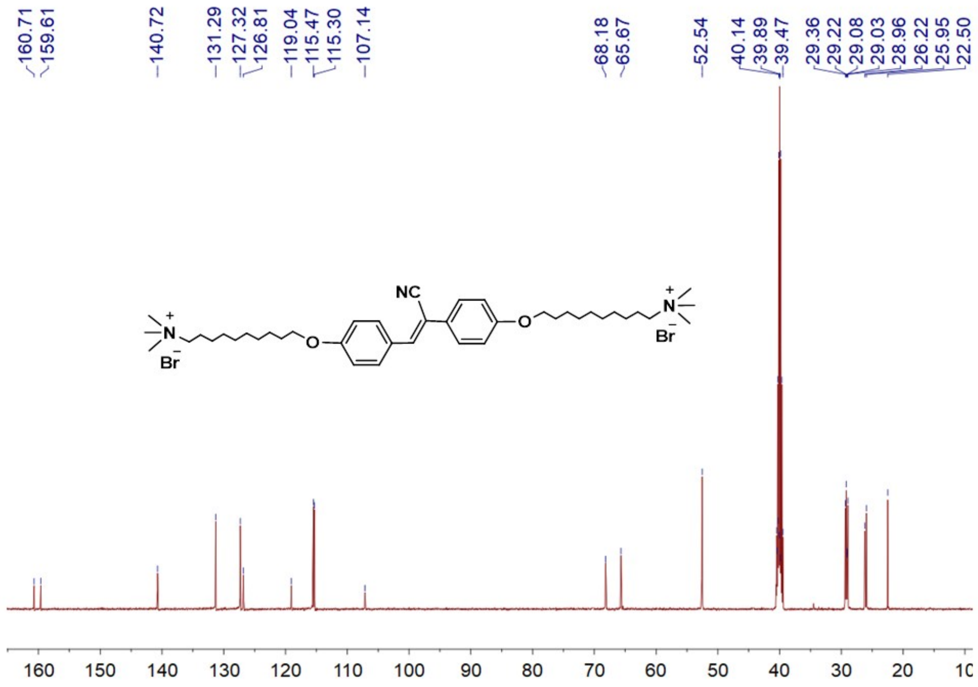

Fig. S9 ^{13}C NMR spectrum (100 MHz, DMSO-d_6, 298 K) of compound **BPT**.

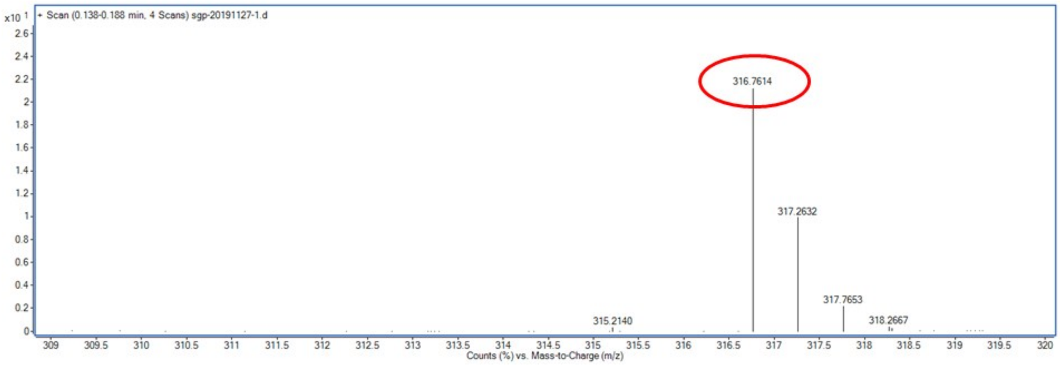

Fig. S10 HR-ESI-MS spectrum of compound **BPT**.

3. Synthesis of model guest molecule[S9]

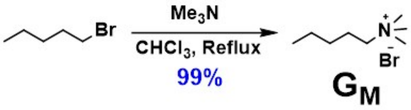

Fig. S11. Synthesis route of model guest molecule $\mathbf{G_M}$.

4. Self-assembly of WP5 with BPT

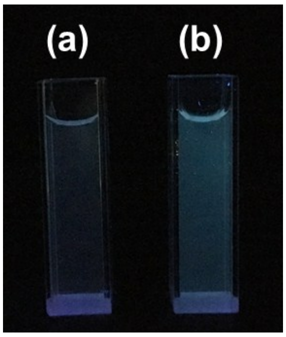

Fig. S12 Fluorescence images: (a) free **BPT** solution and (b) **WP5⊃BPT** nanoparticles. [**WP5**] = 2 × 10^{-5} M and [**BPT**] = 1 × 10^{-4} M, respectively.

5. Tyndall effects of supramolecular nanoparticles

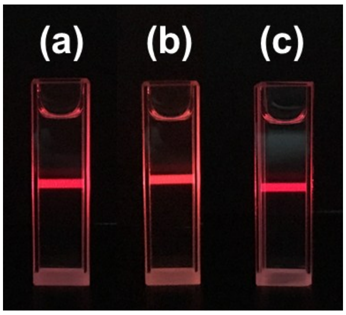

Fig. S13 Tyndall effect: (a) **WP5⊃BPT** nanoparticles, (b) **WP5⊃BPT-DBT** nanoparticles, and (c) **WP5⊃BPT-DBT-NiR** nanoparticles. [**WP5**] = 2 × 10^{-5} M, [**BPT**] = 1 × 10^{-4} M, [**DBT**] = 2.8 × 10^{-7} M, and [**NiR**] = 2.8 × 10^{-7} M, respectively.

6. Determination of the best molar ratio of WP5 and BPT

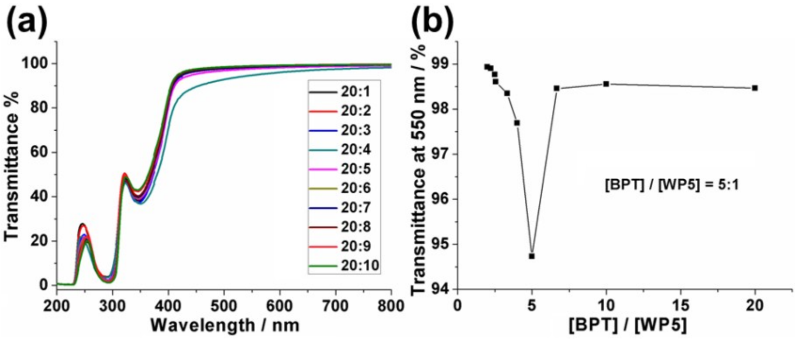

Fig. S14 (a) Optical transmittance of a mixture of **WP5** and **BPT** in water with a constant **BPT** concentration (0.1 mM) on increasing the concentration of **WP5** (0.05 – 0.5 equiv.) at 25 °C. (b) Dependence of the relative optical transmittance at 550 nm on the **WP5** concentration with a fixed concentration of **BPT** (0.1 mM) at 25°C.

7. Determination of the critical aggregation concentration (CAC) of WP5⊃BPT

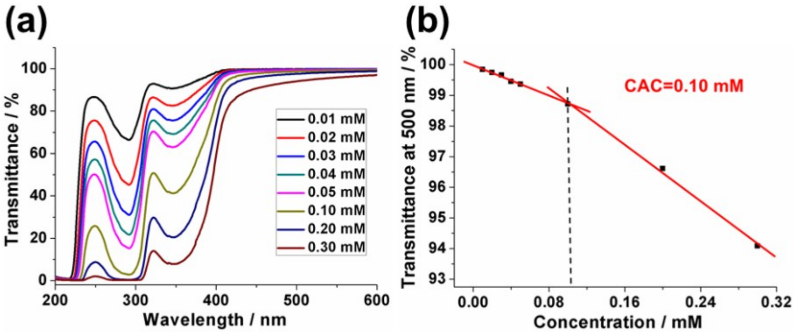

Fig. S15 Optical transmittance of a mixture of **WP5** and **BPT** in water with the best molar ratio of **WP5** and **BPT** (**[BPT]**/**[WP5]** = 5:1) on increasing the concentration of **BPT** (0.01 mM – 0.3 mM) at 25 °C.

8. Zeta potential of supramolecular nanoparticles

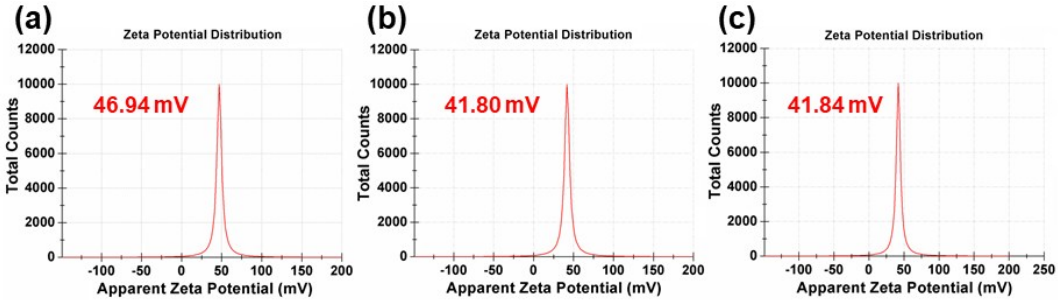

Fig. S16 Zeta-potentials of (a) **WP5⊃BPT** nanoparticles, (b) **WP5⊃BPT-DBT** nanoparticles, and (c) **WP5⊃BPT-DBT-NiR** nanoparticles. [**WP5**] = 2 × 10^{-5} M, [**BPT**] = 1 × 10^{-4} M, [**DBT**] = 2.8 × 10^{-7} M, and [**NiR**] = 2.8 × 10^{-7} M, respectively.

9. Studies on the WP5⊃BPT-DBT-NiR system

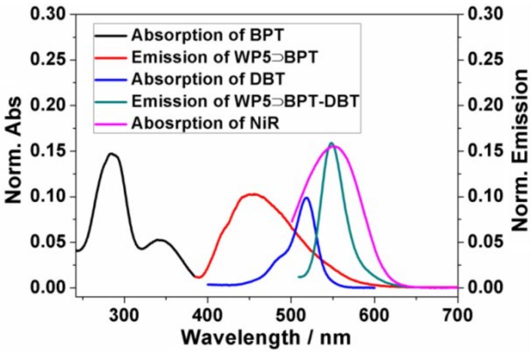

Fig. S17 Normalized absorption and emission spectra of **WP5⊃BPT** (λ_{ex} = 365 nm), **DBT** (λ_{ex} = 450 nm), and **NiR** (λ_{ex} = 540 nm) in water.

10. Fluorescence images of supramolecular nanoparticles

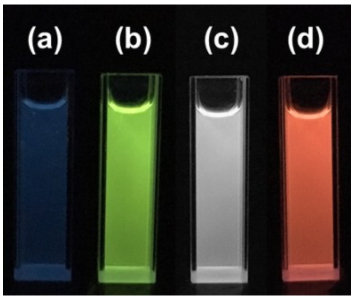

Fig. S18 Fluorescence images: (a) **WP5⊃BPT** nanoparticles, (b) **WP5⊃BPT-DBT** nanoparticles, (c) White light emission, and (d) **WP5⊃BPT-DBT-NiR** nanoparticles.

11. Fluorescence lifetimes of supramolecular nanoparticles

Table S1. Fluorescence lifetimes of **WP5⊃BPT** nanoparticles and **WP5⊃BPT-DBT** nanoparticles monitored at 450 nm upon excitation at 365 nm. [**WP5**] = 2 × 10^{-5} M, [**BPT**] = 1 × 10^{-4} M, and [**DBT**] = 2.8 × 10^{-7} M, respectively.

Sample	τ_1/ns	Rel/%	τ_2/ns	Rel/%	τ/ns	χ^2
WP5⊃BPT	0.60	33.75	2.80	66.25	2.06	1.213
WP5⊃BPT-DBT	0.40	53.70	2.42	46.30	1.34	1.150

Table S2. Fluorescence lifetimes of **WP5⊃BPT-DBT** nanoparticles and **WP5⊃BPT-DBT-NiR** nanoparticles monitored at 550 nm upon excitation at 365 nm. [**WP5**] = 2 × 10^{-5} M, [**BPT**] = 1 × 10^{-4} M, [**DBT**] = 2.8 × 10^{-7} M, and [**NiR**] = 2.8 × 10^{-7} M, respectively.

Sample	τ_1/ns	Rel/%	τ_2/ns	Rel/%	τ/ns	χ^2
WP5⊃BPT-DBT	1.36	35.10	2.82	64.90	2.31	1.042
WP5⊃BPT-DBT-NiR	1.11	53.96	2.38	46.04	1.69	1.101

12. Fluorescence quantum yield of supramolecular nanoparticles

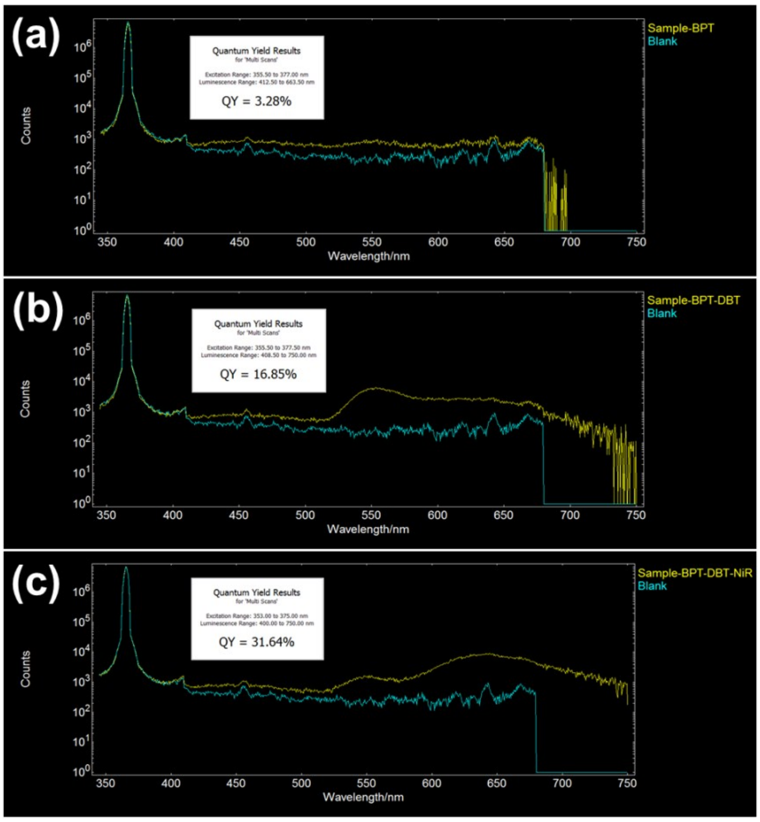

Fig. S19 Absolute fluorescence quantum yields ($\Phi_{f(abs)}$) of (a) **WP5⊃BPT** nanoparticles, (b) **WP5⊃BPT-DBT** nanoparticles, and (c) **WP5⊃BPT-DBT-NiR** nanoparticles upon excitation at 365 nm in aqueous solution. [**WP5**] = 2 × 10^{-5} M, [**BPT**] = 1 × 10^{-4} M, [**DBT**] = 2.8 × 10^{-7} M, and [**NiR**] = 2.8 × 10^{-7} M, respectively.

13. Energy transfer efficiency calculation

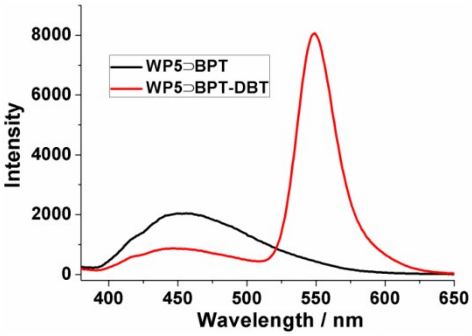

Fig. S20 Fluorescence spectra of **WP5⊃BPT** and **WP5⊃BPT-DBT** ([**WP5**] = 2 × 10^{-5} M, [**BPT**] = 1 × 10^{-4} M, and [**DBT**] = 2.8 × 10^{-7} M, respectively).

The energy-transfer efficiency (Φ_{ET}) was calculated using equation S1:

$\mathbf{\Phi_{ET} = 1 - I_{DA} / I_D}$ (eq. S1)

Where $\mathbf{I_{DA}}$ and $\mathbf{I_D}$ are the fluorescence intensities of the emission of **WP5⊃BPT-DBT** nanoparticles (donor and acceptor) and **WP5⊃BPT** nanoparticles (donor), respectively when excited at 365 nm.

The energy-transfer efficiency (Φ_{ET}) was calculated as 60.9% in water, measured under the condition of [**WP5**] = 2 × 10^{-5} M, [**BPT**] = 1 × 10^{-4} M, [**DBT**] = 2.8 × 10^{-7} M, and λ_{ex} = 365 nm.

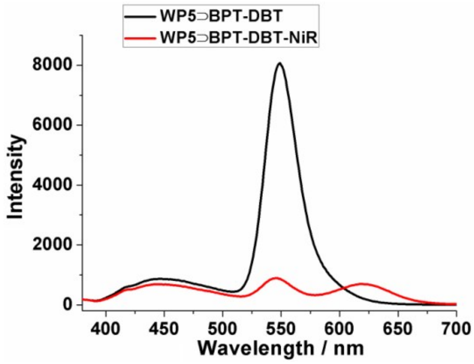

Fig. S21 Fluorescence spectra of **WP5⊃BPT-DBT** and **WP5⊃BPT-DBT-NiR** ([**WP5**] = 2 × 10^{-5} M, [**BPT**] = 1 × 10^{-4} M, [**DBT**] = 2.8 × 10^{-7} M, and [**NiR**] = 2.8 × 10^{-7} M, respectively).

The energy-transfer efficiency (Φ_{ET}) was calculated using equation S2:

$\mathbf{\Phi_{ET} = 1 - I_{DA} / I_D}$ (eq. S2)

Where $\mathbf{I_{DA}}$ and $\mathbf{I_D}$ are the fluorescence intensities of the emission of **WP5⊃BPT-DBT-NiR** nanoparticles (donor and acceptor) and **WP5⊃BPT-DBT** nanoparticles (donor), respectively when excited at 365 nm.

The energy-transfer efficiency (Φ_{ET}) was calculated as 89.4% in water, measured under the condition of [**WP5**] = 2 × 10^{-5} M, [**BPT**] = 1 × 10^{-4} M, [**DBT**] = 2.8 × 10^{-7} M, [**NiR**] = 2.8 × 10^{-7} M, and λ_{ex} = 365 nm.

14. Antenna effect (AE) calculation

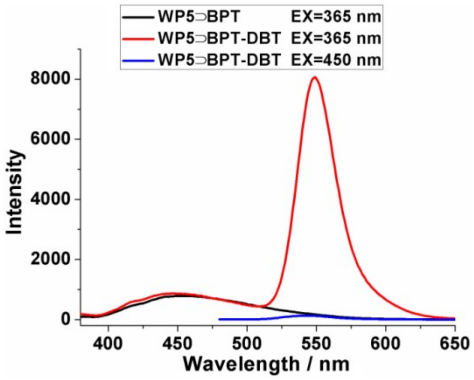

Fig. S22 Fluorescence spectra of **WP5⊃BPT-DBT** in water (red line), blue line (acceptor emission, λ_{ex} = 550 nm) ([**WP5**] = 2 × 10^{-5} M, [**BPT**] = 1 × 10^{-4} M, and [**DBT**] = 2.8 × 10^{-7} M, respectively). The black line represents the fluorescence spectrum of **WP5⊃BPT**, which was normalized according to the fluorescence intensity at 450 nm of the red line.

The antenna effect (AE) was calculated based on the excitation spectra using equation S3.

AE = ($\mathbf{I_{DA,365} – I_{D,365}}$) / $\mathbf{I_{DA,450}}$ (eq. S3)

Where $\mathbf{I_{DA,365}}$ and $\mathbf{I_{DA,450}}$ are the fluorescence intensities at 550 nm with the excitation of the donor at 365 nm and the direct excitation of the acceptor at 450 nm, respectively. $\mathbf{I_{D,365}}$ is the fluorescence intensity at 550 nm of the **WP5⊃BPT** assembly, which was normalized with the **WP5⊃BPT-DBT** assembly at 450 nm.

The antenna effect value was calculated as 47.8 in water, measured under the condition of [**WP5**] = 2 × 10^{-5} M, [**BPT**] = 1 × 10^{-4} M, and [**DBT**] = 2.8 × 10^{-7} M, respectively.

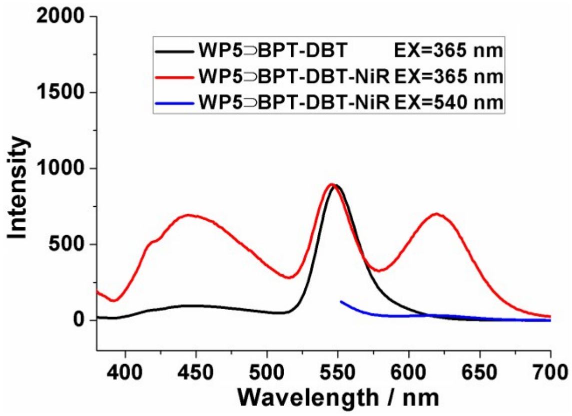

Fig. S23 Fluorescence spectra of **WP5⊃BPT-DBT-NiR** in water (red line), blue line (acceptor emission, λ_{ex} = 540 nm) ([**WP5**] = 2 × 10^{-5} M, [**BPT**] = 1 × 10^{-4} M, [**DBT**] = 2.8 × 10^{-7} M, and [**NiR**] = 2.8 × 10^{-7} M, respectively). The black line represents the fluorescence spectrum of **WP5⊃BPT-DBT**, which was normalized according to the fluorescence intensity at 550 nm of the red line.

The antenna effect (AE) was calculated based on the excitation spectra using equation S4.

AE = ($\mathbf{I_{DA,365} – I_{D,365}}$) / $\mathbf{I_{DA,540}}$ (eq. S4)

Where $\mathbf{I_{DA,365}}$ and $\mathbf{I_{DA,540}}$ are the fluorescence intensities at 620 nm with the excitation of the donor at 365 nm and the direct excitation of the acceptor at 540 nm, respectively. $\mathbf{I_{D,365}}$ is the fluorescence intensity at 620 nm of the **WP5⊃BPT-DBT** assembly, which was normalized with the **WP5⊃BPT-DBT-NiR** assembly at 550 nm.

The antenna effect value was calculated as 20.1 in water, measured under the condition of [**WP5**] = 2 × 10^{-5} M, [**BPT**] = 1 × 10^{-4} M, [**DBT**] = 2.8 × 10^{-7} M, and [**NiR**] = 2.8 × 10^{-7} M, respectively.

15. Fluorescent studies on white light emission

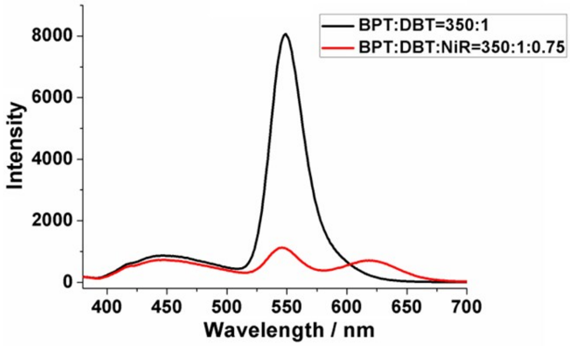

Fig. S24 Fluorescence spectra of **WP5⊃BPT-DBT** and **WP5⊃BPT-DBT-NiR** ([**WP5**] = 2 × 10^{-5} M, [**BPT**] = 1 × 10^{-4} M, [**DBT**] = 2.8 × 10^{-7} M, and [**NiR**] = 2.1 × 10^{-7} M, respectively).

The energy-transfer efficiency (Φ_{ET}) was calculated using equation S5:

$\mathbf{\Phi_{ET} = 1 - I_{DA} / I_D}$ (eq. S5)

Where $\mathbf{I_{DA}}$ and $\mathbf{I_D}$ are the fluorescence intensities of the emission of **WP5⊃BPT-DBT-NiR** nanoparticles (donor and acceptor) and **WP5⊃BPT-DBT** nanoparticles (donor), respectively when excited at 365 nm.

The energy-transfer efficiency (Φ_{ET}) was calculated as 86.5% in water, measured under the condition of [**WP5**] = 2 × 10^{-5} M, [**BPT**] = 1 × 10^{-4} M, [**DBT**] = 2.8 × 10^{-7} M, [**NiR**] = 2.1 × 10^{-7} M, and λ_{ex} = 365 nm.

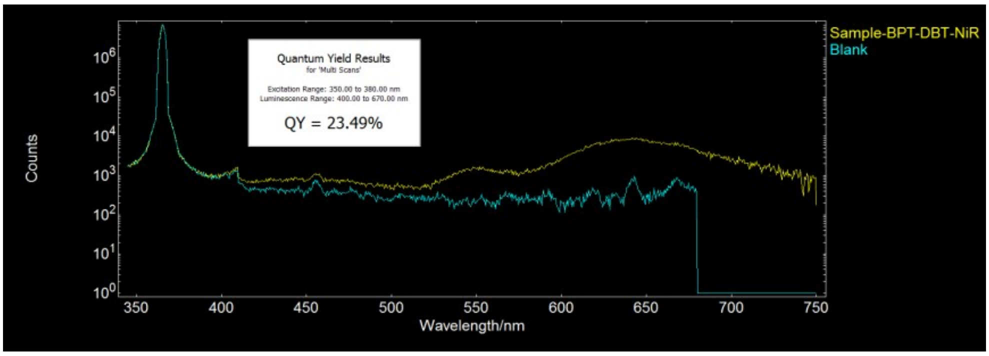

Fig. S25 Absolute fluorescence quantum yields ($\Phi_{f(abs)}$) of **WP5⊃BPT-DBT-NiR** nanoparticles upon excitation at 365 nm in aqueous solution. [**WP5**] = 2 × 10^{-5} M, [**BPT**] = 1 × 10^{-4} M, [**DBT**] = 2.8 × 10^{-7} M, and [**NiR**] = 2.1 × 10^{-7} M, respectively.

16. Fluorescence images of supramolecular nanoparticles

(A) The first-step energy transfer: BPT → DBT

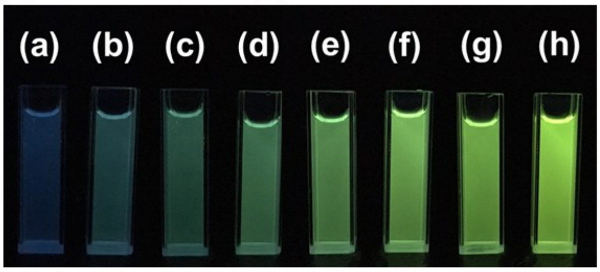

(B) The second-step energy transfer: DBT → NiR

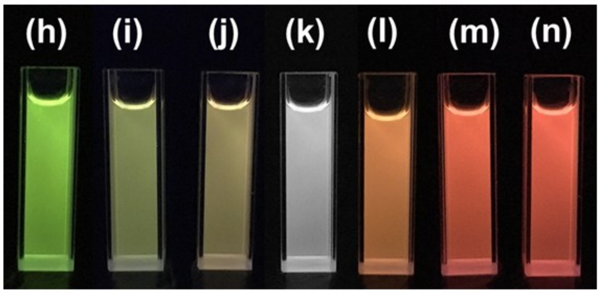

Fig. S26 Fluorescence images: (A) **WP5⊃BPT-DBT** nanoparticles ([**WP5**] = 2×10^{-5} M and [**BPT**] = 1×10^{-4} M) with different concentration of **DBT**: (a) 0 M, (b) 1.5×10^{-8} M, (c) 3.3×10^{-8} M, (d) 4×10^{-8} M, (e) 8×10^{-8} M, (f) 1.1×10^{-7} M, (g) 2×10^{-7} M, and (h) 2.8×10^{-7} M, respectively; (B) **WP5⊃BPT-DBT-NiR** nanoparticles ([**WP5**] = 2×10^{-5} M, [**BPT**] = 1×10^{-4} M, and [**DBT**] = 2.8×10^{-7} M) with different concentration of **NiR**: (h) 0 M, (i) 7.3×10^{-8} M, (j) 1.5×10^{-7} M, (k) 2.1×10^{-7} M, (l) 2.6×10^{-7} M, (m) 4.4×10^{-7} M, and (n) 5.8×10^{-7} M, respectively.

17. Fluorescent studies on the WP5⊃BPT-NiR system

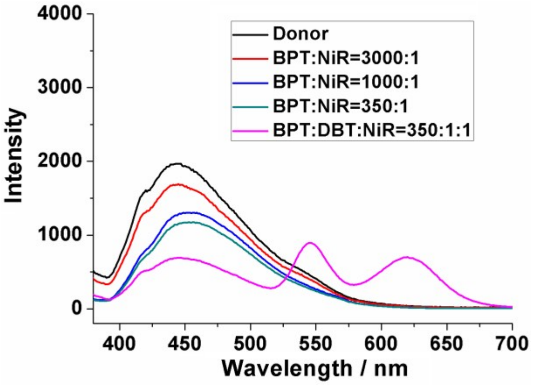

Fig. S27 Fluorescent spectra of **WP5⊃BPT** nanoparticles in water with different concentrations of **NiR** and **DBT**.

18. References

S1. H. Li, D.-X. Chen, Y.-L. Sun, Y. Zheng, L.-L. Tan, P. S. Weiss and Y.-W. Yang, *J. Am. Chem. Soc.*, 2013, **135**, 1570–1576.

S2. T. Ogoshi, S. Kanai, S. Fujinami, T.-A. Yamagishi and Y. Nakamoto, *J. Am. Chem. Soc.*, 2008, **130**, 5022–5023.

S3. D. Cao, Y. Kou, J. Liang, Z. Chen, L. Wang and H. Meier, *Angew. Chem. Int. Ed.*, 2009, **48**, 9721–9723.

S4. T. Ogoshi, M. Hashizume, T.-A. Yamagishi and Y. Nakamoto, *Chem. Commun.*, 2010, **46**, 3708–3710.

S5. Y. Ma, X. Ji, F. Xiang, X. Chi, C. Han, J. He, Z. Abliz, W. Chen and F. Huang, *Chem. Commun.*, 2011, **47**, 12340–12342.

S6. C. Li, X. Shu, J. Li, S. Chen, K. Han, M. Xu, B. Hu, Y. Yu and X. Jia, *J. Org. Chem.*, 2011, **76**, 8458–8465.

S7. M. K. Dhinakaran, W. Gong, Y. Yin, A. Wajahat, X. Kuang, L. Wang and G. Ning, *Polym. Chem.*, 2017, **8**, 5295–5302.

S8. J.-J. Li, Y. Chen, N. Cheng and Y. Liu, *Adv. Mater.*, 2017, **29**, 1701905–1701909.

S9. G. Sun, Z. He, M. Hao, M. Zuo, Z. Xu, X.-Y. Hu, J.-J. Zhu and L. Wang, *J. Mater. Chem. B*, 2019, **7**, 3944–3949.